Escherichia coli Diacylglycerol Kinase Is an α-Helical Polytopic Membrane Protein and Can Spontaneously Insert into Preformed Lipid Vesicles†

Charles R. Sanders II,*,‡ Lech Czerski,‡ Olga Vinogradova,‡ Prakash Badola,‡ David Song,§ and Steven O. Smith§

Department of Physiology and Biophysics, Case Western Reserve University, Cleveland, Ohio 44106-4970, and Department of Molecular Biophysics and Biochemistry, Yale University, Box 208114, New Haven, Connecticut 06520

Received February 28, 1996; Revised Manuscript Received May 6, 1996⊗

ABSTRACT: *Escherichia coli* diacylglycerol kinase (DAGK) is a 13.2 kDa enzyme which spans the cytoplasmic membrane three times. Functional DAGK was purified to homogeneity using a polyhistidine tag and Ni(II)-chelate chromatography. Transmission Fourier transform infrared spectroscopy (FT-IR) of DAGK in phosphatidylcholine multilayers led to the conclusion that ≥90 of DAGK's native 121 residues are α-helical, consistent with a model in which DAGK consists of two amphipathic α-helices and three transmembrane helices. Polarized attenuated total reflection FT-IR studies of DAGK in oriented multilamellae yielded data consistent with a topological arrangement in which the three transmembrane helices are well-aligned with the bilayer normal while the two amphipathic helices are approximately parallel with the membrane plane. The ability of DAGK to spontaneously insert into preformed lipid vesicles was examined using a novel assay system involving DAGK-catalyzed phosphorylation of a fluorescently tagged diacylglycerol. When micellar DAGK is diluted into L_α-phase vesicles spontaneous insertion of the enzyme is fairly efficient (ca. 30%). DAGK refolding and insertion from delipidated urea-solubilized DAGK into lipid vesicles is also modestly efficient (3.8 ± 2.1%) above the gel to liquid crystalline phase transition temperature. The insertion studies indicate that the difference in energy barriers ($\Delta\Delta G^{\ddagger}$) between pathways leading to catalytically productive folding and insertion of DAGK relative to unproductive pathways is <4 kcal/mol. However, additional studies carried out with mutant forms of DAGK indicated that the differences between refolding/insertion pathways for DAGK *in vivo* and *in vitro* can be significant.

Microbial diacylglycerol kinase (DAGK) is a small (ca. 13 kDa) membrane protein which catalyzes the phosphorylation of diacylglycerol by MgATP (Walsh & Bell, 1992; Russ et al., 1988). Based on gene fusion experiments in which a series of truncated DAGKs were expressed in *Escherichia coli* as chimeras with topological reporter proteins, it is known that the enzyme spans the cytoplasmic membrane three times (Smith et al., 1994). In this study we carried out experiments designed to elucidate DAGK's secondary structure and to provide insight into the means by which DAGK can be productively inserted into lipid bilayers.

The structure and mechanism of DAGK is of interest for a variety of reasons. DAGK is known to be essential to the survival of gram-negative bacteria under conditions of low osmolarity (Yamashita et al., 1993; Raetz & Newman, 1978). As an integral membrane protein involved in lipid metabolism, DAGK is representative of an entire class of enzymes for which relatively little is known on the molecular level (Bell & Hjelmstad, 1991). Investigation of the means by which DAGK inserts into lipid bilayers is of interest not only because of its specific relevance to DAGK but also because information gleaned for DAGK may be of more general relevance for understanding the biologically ubiquitous processes of membrane protein insertion (Gennis, 1989; Wickner et al., 1991; von Heijne, 1994; Popot et al., 1994; Schatz & Dobberstein, 1996).

E. coli DAGK was recently recloned and overexpressed with a polyhistidine purification tag by James Bowie and his co-workers at UCLA (unpublished) such that milligram quantities of the pure enzyme can now be routinely purified to homogeneity, setting the stage for detailed molecular characterization. In this paper, we report infrared spectroscopic studies of reconstituted DAGK to establish its secondary structural content and to establish constraints upon possible orientations of discrete secondary structural elements with respect to the membrane bilayer. We also describe use of a novel DAGK assay to establish whether the enzyme can autoinsert from either micelles or urea solutions into preformed lipid vesicles. Finally, we describe experiments employing DAGK mutants designed to shed some light upon the possible relevance of the results from the vesicle insertion studies to the process of DAGK refolding and insertion *in vivo*.

MATERIALS AND METHODS

Purification of DAGK. Tagged DAGK was overproduced in *E. coli* strain WH1061 harboring the inducible plasmid pSD0004 (J. Bowie, unpublished). The sequence of the tag, which replaces the N-terminal Met of the 122-residue native DAGK, is MGHHHHHHEL. Cells were grown in Luria broth medium and induced with isopropyl thiogalactoside

† This work was supported by the federal government of the U.S.A. (NIH, GM47485 to C.R.S. and GM46732 to S.O.S.). C.R.S. is an established investigator of the American Heart Association (AHA 94001540). Support for O.V. was provided via an NIH training grant (T32 DK07678).

* Corresponding author. Telephone: (216)-368-8651. Internet: crs4@po.cwru.edu.

‡ Case Western Reserve University.

§ Yale University.

⊗ Abstract published in *Advance ACS Abstracts,* June 15, 1996.

S0006-2960(96)00489-8 CCC: $12.00

according to standard methods. Harvested cells (typically about 3 g wet from a liter of culture) were suspended in a pH 7.5 buffer (50 mM Tris, 0.1 M NaCl) and lysed by standard methods involving sonication and lysozyme/deoxyribonuclease treatment. Following lysis, the pH of the lysed suspension was adjusted to pH 7.5−8.0. The zwitterionic detergent Empigen (*n*-dodecyl-*N*,*N*-dimethylglycine, Calbiochem, San Diego, CA) was then added to a concentration of 3%. To this solution was added Ni(II)-agarose resin (Qiagen, Chatworth, CA) at a level of 1.2 mL of packed resin for every gram of wet cells. The solution and nickel resin were tumbled overnight at 4 °C followed by filtration of the resin, which was then washed with 3% empigen in 50 mM phosphate and and 300 mM NaCl, pH 7.5. Non-polyHis tagged material was eluted from the column using 1.5% empigen in the above buffer plus 40 mM imidazole. The column was then equilibrated with 1% decyl maltoside (DM, Anatrace, Maumee, OH) in water followed by elution with 1% DM plus either 0.3 M imidazole (pH 7.9) or 0.4 M ammonium hydroxide (not buffered). The protein eluted as a visible band at the interface between the equilibration and elution solutions and could thus be collected in a highly concentrated form (10−30 mg/mL). No difference in specific DAGK activity (units/mg, see below) was found for the enzyme eluted by NH_4OH or imidazole. DAGK is completely stable in both ammonia and imidazole-containing DM solutions for at least a few hours, although some loss of activity occurs over a period of days for DAGK in the more basic ammonia solution. The advantage of using ammonia to elute DAGK is that it can be removed during lyophilization of the enzyme. We occasionally used 3% *n*-octyl β-glucoside or Empigen instead of 1% DM in the final equilibration and elution steps, but normally preferred DM because DAGK is more stable and less prone to aggregation in decyl maltoside micelles relative to other detergents.

DM solutions of purified DAGK were frozen in liquid N_2 and then lyophilized to produce an easily handled powder (containing 10−35% DAGK by weight) which can be redissolved in the buffer of choice with little (<15%) or no loss of enzyme activity relative to the prelyophilized solution.

DAGK purified by the above method was judged to be >95% pure by SDS−PAGE (DAGK must not be boiled or it irreversibly oligomerizes) and by proton NMR (data not shown). Of the impurities which can be observed on overloaded gels, none appear to be present in amounts higher than 1%.

In this study, DAGK was quantitated based upon either its absorbance at 280 nm (assuming an $\epsilon_{1.0\ mg/mL}$ of 2.1 optical density units calculated based on DAGK's sequence) or upon its activity in the coupled mixed micellar assay under standard conditions (below) assuming an observed specific activity for the pure enzyme of 15 units/mg.

In kinetic characterization of polyHis-tagged DAGK (unpublished work), we have not detected dramatic differences between the properties of the tagged enzyme and those of the native enzyme (Walsh & Bell, 1986a,b). With regard to its possible perturbation of bilayer insertion experiments, it should be pointed out that (i) the N-terminal cytoplasmic domain of native DAGK bears a net positive charge which will remain positive in the presence of the polyHis tag, (ii) the presence of the tag does not appear to perturb DAGK insertion *in vivo* (Wen et al., 1996), and (iii) the polyHis tag of bilayer-associated DAGK appears to exist in mobile, unstructured conformation as shown by high speed H1 magic angle spinning NMR (Sanders, unpublished) suggesting it is truly passive in terms of perturbing DAGK's protein−bilayer interactions. Given the above considerations, no attempt was made to remove the tag. All studies reported in this paper involve the polyHis-tagged enzyme. DAGK mutants (Wen et al., 1996) were purified from strains also provided to us by the Bowie lab using the same procedure as for the wild type.

Reconstitution of DAGK in Lipid Vesicles and Preparation of IR Samples. Purified DAGK in a 1% (21 mM) DM solution or in 3% *n*-octyl β-glucoside solution was mixed with mixed micellar solutions containing 100 mM lipid (DPPC or POPC) and 300 mM octyl glucoside. The mol/mol ratio of DAGK/lipid was fixed at 1:100. Detergent was then removed resulting in DAGK-containing multilamellar vesicles (MLV) by either (i) extensive dialysis for several days and several changes of buffer solution at 4 °C, or (ii) >20× dilution of the concentrated mix into detergent-free buffer followed by (repeated) centrifugation and rinsing of the multilamellar vesicles. DAGK activity was measured before and after reconstitution to insure negligible loss of activity during the process. The DAGK-containing multilamellar suspensions could be frozen and thawed, or frozen, lyophilized, and rehydrated, without significant loss of DAGK activity. For polarized attenuated reflectance Fourier transform infrared spectroscopy (ATR-IR), about 0.25 mL of MLV dispersions containing roughly 10 nmol of DAGK and 1 μmol of lipid was spread near one 20 mm end of a 52 × 20 × 2 mm Ge internal reflection element and partially dried using a flow of N_2 in the direction of the long side of the plate to form an oriented multilamellar lipid-DAGK film of roughly 1 cm^2. As mentioned above, DAGK can be dried and rehydrated without loss of activity. As a result, we assume that the structure and orientation of the protein does not change significantly upon drying. With a transmembrane topology, DAGK may be more stable to changes in hydration than small membrane-associated peptides such as melittin (Frey & Tamm, 1991). Assuming that each lipid in the multilayers occupies roughly 65 $Å^2$ of surface area (Lewis & Engelman, 1983), it can be estimated that these films are, on the average, roughly 2000 bilayers thick [12 μm assuming a 60 Å spacing (Rand & Parsegian, 1989)]. For transmission Fourier transform infrared spectroscopy (FT-IR), a similar procedure was followed except that 50 μL of sample was dried on a 12.7 × 1 mm Ge window.

Fourier Transform IR Methods and Theory. The IR experiments of this study were carried out using a Nicolet Magna 550 spectrometer. The experimental methods and related data processing and have been described previously (Arkin et al., 1995). In the polarized ATR experiments, the dichroic ratio [defined as the ratio between absorption of parallel ($A_\parallel$) and perpendicular ($A_\perp$) polarized light, $R^{ATR} = A_\parallel/A_\perp$] is used to calculate an order parameter (S) defined as

$$S = \langle 3\cos^2\theta - 1\rangle/2 = 2(E_x^2 - R^{ATR}E_y^2 + E_z^2)/[(3\cos^2\alpha - 1)(E_x^2 - R^{ATR}E_y^2 - 2E_z^2)] \quad (1)$$

where θ is the angle between the helix director and the normal of the internal reflection element, α is the angle between the helix director and the transition dipole moment of the amide I vibrational mode, and $E_{x,y,z}$ are the electric field amplitudes of the evanescent wave given by Harrick

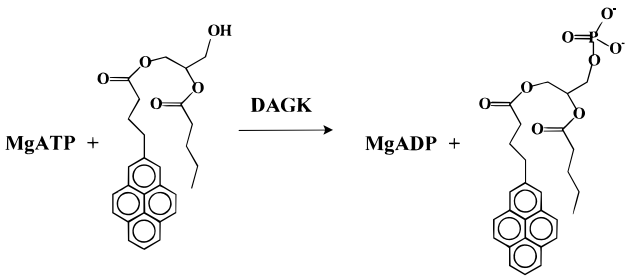

FIGURE 1: DAGK reaction involving pyrene-tagged diacylglycerol (PBBG) to produce phosphatidic acid (PBBPA). PBBG and PBBPA are readily separated by thin layer chromatography and quantitated by their fluorescent emission intensity as described in Materials and Methods section.

(1967). The choice of α is currently a matter of controversy (Axelsen et al., 1995). Rather than trying to choose among the various literature possibilities, we have instead calculated a *range* of order parameters using α ranging from 25° to 39° with the low end value being based on more recent estimates (Axelsen et al., 1995; Bradbury et al., 1962; Tsuboi, 1961).

In cases where there are a population of *n* values of θ represented by the measured dichroic ratio, the order parameter can be more explicitly defined as

$$S = [\sum_n P_n(3\cos^2\theta_n - 1)]/2 \qquad (2)$$

where P_n represents the fractional population of the *n*th state (sum of all $P = 1$).

Coupled Assay of DAGK's Activity. For routine quantitation of DAGK's activity during purification and sample preparation, we developed a spectrophotometric assay in which the production of ADP by DAGK-catalyzed phosphorylation of DAG is coupled to NADH oxidation via the mediation of pyruvate kinase and lactic dehydrogenase. The DAG actually used in this assay is *sn*-1,2-dihexanoylglycerol and purified DAGK generally exhibits a specific activity under apparent V_{max} conditions (concentration of both substrates > K_m) of 15 units/mg of DAGK (1 unit = 1 μmol phosphatidic acid produced per minute). The details of this assay will be published elsewhere. However, it should be noted that this assay is not appropriate for solutions which are not optically transparent (e.g., large vesicles or MLV), where compartmental (e.g., outside vs inside of a vesicle) activity is of interest, or where buffer components (e.g., urea) would interfere with the activities of the water-soluble coupling enzymes.

Synthesis of a Fluorescently Tagged Diacylglycerol. For the purposes of this study it was necessary to be able to directly quantitate concentrations of both DAG *and* phosphatidic acid (PA) during various time points of a DAGK reaction, something which is not possible with either the coupled assay or the P32-based assay (Walsh & Bell, 1992). We thus sought to synthesize a diacylglycerol which could be easily quantitated via fluorescence both before and after phosphorylation. For this purpose the previous characterization of DAGK's diglyceride specificity (Walsh et al., 1990) proved very helpful. Based on those results, it was reasoned that the compound 1-pyrenebutyrl-2-butyryl-*sn*-glycerol (PBBG) should prove to be a good substrate for DAGK (Figure 1). Additional considerations in the choice of this compound were (1) pyrene is completely hydrophobic, and (2) the short chain at the *sn*-2 position is long enough to ensure bilayer anchoring (Schwonek & Sanders, 1993), yet short enough such that the extra volume occupied by the pyrene moiety at the 1-position (relative to a more conventional acyl chain) can be accommodated without disruption of the host bilayer.

3-Benzyl-*sn*-glycerol and pyrenebutyric acid were purchased from Sigma (St. Louis, MO) and from Aldrich (Milwaukee, WI), respectively. Pyrenebutyric acid was converted into its acyl chloride and reacted stoichiometrically with 3-benzyl glycerol to form *sn*-1-pyrenebutyryl-3-benzyl glycerol which was purified by flash chromatography. This intermediate was then acylated at the 2-glycero position with butyric anhydride and the product 1-pyrenebutyryl-2-butyryl-3-benzylglycerol was purified by flash chromatography and identified by ^{1}H NMR. The benzyl protecting group by then removed by catalytic hydrogenation, and the desired final product, PBBG, was purified by flash chromatography and identified by ^{1}H NMR. Additional details of this synthesis are available upon request.

Thin Layer Chromatography Assay for DAGK. Based upon the work of Walsh et al. (1990), we predicted that the K_m for PBBG as a substrate for DAGK should be about 1 mol % (mol of PBBG/total mol of lipid + detergent × 100). Accordingly, we used 5 mol % PBBG in most assays, a level low enough to ensure that the bilayer properties are dominated by the host lipid rather than by the DAG but high enough to ensure a reaction rate approaching V_{max}.

Attempts to develop a *continuous* assay involving PBBG proved unsuccessful, and so an assay was developed based upon separating PBBG from PBBPA at various time points using TLC, followed by quantitation of the fluorescent intensities of the reactant and products. PBBG was codissolved at a level of 5 mol % with detergent and/or lipid in 95:5 benzene/ethanol and lyophilized. The resulting powder was then hydrated in buffer (50 mM PIPES, 60 mM LiCl, 0.1 mM EGTA, 0.1 mM EDTA, pH 6.7) plus 5 mM ATP and 20 mM Mg^{2+} such that the total lipid + detergent concentration was 25 mM. When the assay was run with mixed micelles, the amphiphile composition was 20 mM decyl maltoside, 4 mM DMPC, and 1.25 mM PBBG. When the assay was vesicular, the composition was 24 mM POPC or DPPC and 1.25 mM PBBG.

Unilamellar vesicles were formed by extruding DPPC or POPC assay mixtures (above paragraph) about 20 times through 100 nm polycarbonate filters using a LIPOSOFAST extruder (Avestin, Ottawa, ON) at temperatures at least 10 °C above T_m (ca. −5 °C for POPC, 40 °C for DPPC). Vesicles formed with or without PBBG were observed to be similar both in the forces required to extrude them and in terms of their light scattering properties. As will be demonstrated later in this paper, lack of vesicle disruption by PBBG is also supported by the fact that there are clearly two equimolar "compartments" (presumably outside and inside) of PBBG and by the fact that the PBBG-containing DPPC vesicles appear to exhibit normal (and distinctive) phase behavior above and below T_m. Attempts to extrude POPC vesicles containing 5 mol % 1,2-dipalmitoyl-*sn*-glycerol provided a contrasting case in which the pressure required for extrusion was much higher that for pure POPC, suggestive of a DAG-induced change in the lipid morphology and/or phase. The DAGK reactions were initiated by adding a relatively small volume of stock DAGK (1−10 μL) to the vesicles or mixed micelles (100−500 μL). At various time intervals 4 μL aliquots were removed and spotted on 7 cm

long silica gel TLC plates (Whatman, K6 Silica gel plates, 250 μm thick, no fluorescent indicator) about 1 cm from the bottom.

All time points from a single reaction were spotted on a *single* plate which was stored at −20 °C while the reaction continued to run. Ideally, four time points representing 0%, 10%, 20%, and 40% extent of reaction were taken. The equilibrium constant for the DAGK reaction is large in the direction of DAG phosphorylation such that initial rate (linear) kinetics persist beyond 50% of DAG conversion. After all time points were spotted, excess DAGK was added and the reaction was allowed to proceed to equilibrium, at which point another 4 μL aliquot was removed and spotted on the same TLC plate as the assay points. TLC plates were then developed with 65:25:2:2 chloroform/methanol/water/formic acid. In this system PBBG exhibits an R_f of about 0.95 while that of the phosphatidic acid product (PBBPA) is about 0.4.

Plates were removed from the TLC chamber, dried, and taken immediately to a dark room and placed under a near-UV lamp to induce light blue fluorescence from the pyrene-labeled PBBG and PBBPA. Digital photographs of these plates were taken with a Kodak Digital Camera 40 (Rochester, NY). The photographs were downloaded onto a computer, and the total intensities of the PBBPA and PBBG spots were quantitated using SigmaScan software (Jandel, San Rafael, CA). The relationship between spot intensity and micromoles of product was determined by dividing the intensity of a time point PBBPA spot with the equilibrium PBBPA spot intensity and comparing that ratio with ratios obtained for standards representing known PBBPA contents. Additional practical details of this assay are available upon request.

RESULTS

Secondary Structure and Orientation of DAGK in Lipid Bilayers. Recent circular dichroism (CD) data taken in our lab and that of J. Bowie (unpublished) has indicated that the secondary structure of catalytically viable DAGK in mixed micelles is highly helical. However, the data are difficult to quantitate due to differential light scattering and uncertainty in the mean residue ellipticity for membrane protein structural elements (Park et al., 1992; Fasman, 1995). For directly probing the secondary structure of DAGK in lipid bilayers, we chose to use IR spectroscopy (Williams, 1994; Braiman & Rothschild, 1988; Surewicz et al., 1993).

The amide I region of the transmission IR spectrum of DAGK is illustrated in Figure 2 along with its Fourier self-deconvolution. The integrated intensity of the 1656 cm^{-1} band in Figure 2B is 66 ± 5% of the total intensity in the 1600−1700 cm^{-1} amide I region. The 5% standard deviation reflects the range observed when this measurement was repeated on eight different runs with several samples. Based upon the work of Veyaminov and Kalnin (1990a,b), it can be estimated that amino acid side chains such as Gln, Asn, Lys, and Arg contribute ca. 8% of the total intensity to the amide I region. This is lower than the "typical" range of 15−20% quoted by Surewicz et al. (1992), suggesting that an estimate of 74 ± 5% represents a *lower limit* for the intensity of the α-helical band relative to the total backbone amide I intensity. This estimate argues that at least 90 of 131 residues of tagged DAGK occur in α-helices assuming that the normalized per residue contributions to the amide I

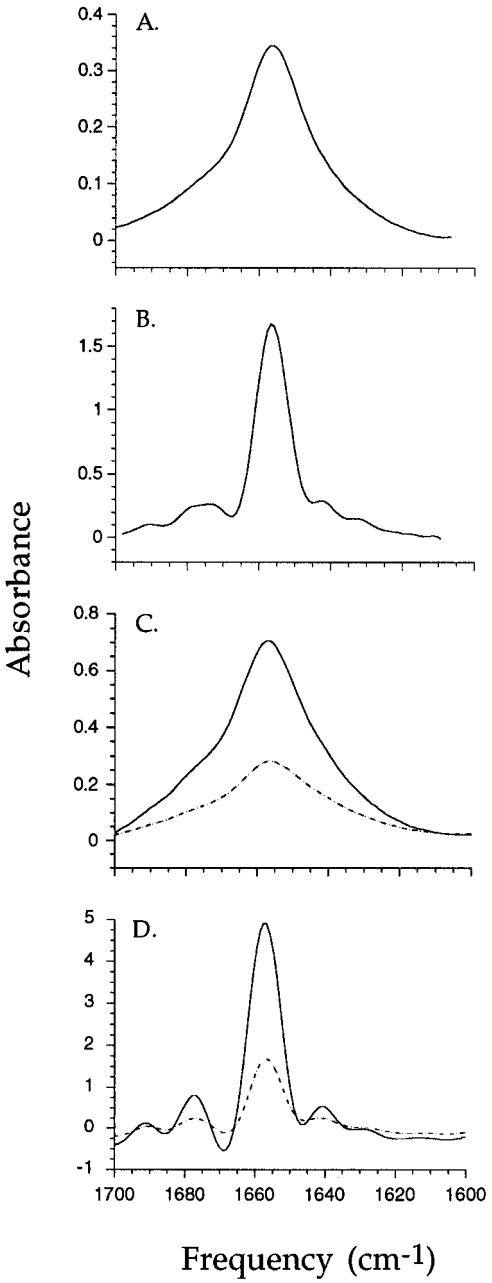

FIGURE 2: Fourier transform infrared spectra of DAGK in membrane bilayers. Each spectrum represents the average of 1000 scans acquired at a resolution of 4 cm^{-1} and processed using automatic baseline correction. (A) Amide I region of transmission FT-IR of DAGK in POPC bilayers at 25 °C. (B) Fourier self-deconvolution of A using a bandwidth of 13 cm^{-1} and an enhancement of 2.4 with Happ−Genzel apodization (Kauppinen et al., 1981; Arkin et al., 1995). (C) Polarized ATR-IR spectra of DAGK in DPPC bilayers at 25 °C obtained with parallel (solid line) and perpendicular (dashed line) polarized light. (D) Fourier self-deconvolution of C using a bandwidth of 13 cm^{-1} and enhancement of 2.4 with Happ−Genzel apodization.

intensity are roughly the same for different secondary structural elements. The measurements of Veyaminov and Kalnin (1990a,b) support this assumption for β-sheets and α-helices.

These ≥90 α-helical residues must almost certainly be placed within the C-terminal 121 residues of the recombinant enzyme since the first 10 residues of the DAGK used in these studies are in the polyHis tag. High speed (14.1 kHz) magic angle spinning proton NMR of DAGK in hydrated POPC MLV at 25 °C indicates that the polyHis tag is disordered (data not shown). This would leave 24 ± 7 residues in the

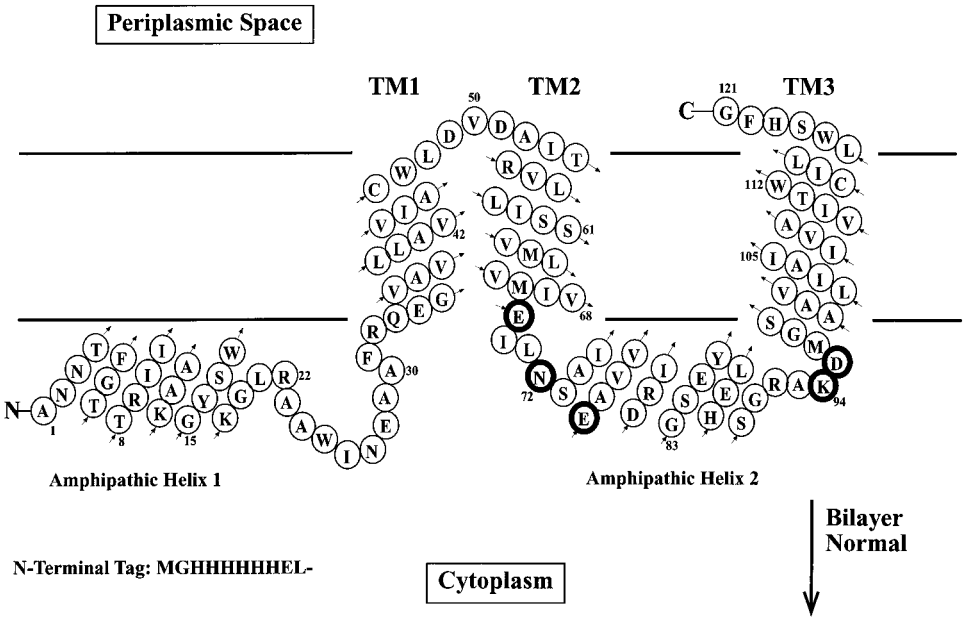

FIGURE 3: Model for DAGK's topology, secondary structure, and probable helical orientations based on experimental data and other considerations presented in this paper and elsewhere (Smith et al., 1994). The exact beginnings and ends of the helices are putative, and it is not known whether the cytoplasmic helices clear the membrane surface (as shown) or are partially embedded in the lipid water interface. While Arg55 may lie slightly within the apolar phase (as shown), its side chain likely forms an ion pair with Asp51 and/or "snorkles" to more polar regions of the interface. Emboldened residues are those which have been observed to be fully conserved both evolutionarily and in mutagenesis studies (Wen et al., 1996). This model should not be taken to imply anything about DAGK's tertiary structure. It should also be pointed out that the active form of DAGK is probably homooligomeric (Bowie and Sanders, unpublished results).

sequence proper which are not α-helical. Determination of ≥90 α-helical residues for DAGK is consistent with a model for the enzyme which includes five helical segments. It has previously been suggested that there are amphipathic α-helices near the N-terminus and in the region linking TM segments 2 and 3 based upon (i) combined analysis of helical wheel diagrams and multiple aligned sequences (Smith et al., 1994), (ii) extensive mutagenesis studies (Wen et al., 1996), and (iii) the presence of potential N-cap motifs (Harper & Rose, 1993; Reithmeier, 1995) near the N-termini of the two putative helical segments (**N**NT**T** and **S**AI**E**). Assuming these two regions do indeed encompass helices 15−30 residues in length, the IR results suggest that at least two and possibly all three of the TM segments are also α-helical. TM segment 2 is almost certainly helical based upon the existence of a well-conserved N-cap motif (**D**AI**T**) at its N-terminus. TM segment 3 is also likely to be α-helical: it has the longest stretch of apolar residues of the three TM segments (ca. 23 residues) and is also initiated by a potential N-cap motif (**D**MG**S**). While the 15 residue hydrophobic stretch of TM segment 1 is a little shorter than that of a typical TM helix, it is probably still long enough to span the bilayer (Adams and Rose, 1985). In addition, recent mutagenesis studies (Wen et al., 1996) have shown that residues 37, 41, and 45 (all Ala) of this segment were the only residues within this segment which were functionally intolerant of replacement by another (i.e. slightly larger) apolar amino acid. The need for Ala (a strong helical promoter) at these positions and the periodicity of 4 both support assignment of this segment as an α-helix. The approximate sequential locations of the five probable helical segments of DAGK are shown in Figure 3.

Amide exchange can be used to assess the accessibility of the amide protons of DAGK to water. The amide II vibrational band at 1542 cm^{-1} is significantly shifted following 0.5−25 h of deuterium exchange for the backbone NH proton. The observed decrease of intensity of the 1542 cm^{-1} band of 27 ± 11% is consistent with 20−50 solvent-exposed residues, 10 of which will be in the polyHis purification tag.

Some constraints upon possible orientations of the five putative helical segments of DAGK can be established by polarized ATR-IR spectroscopy (Axelsen et al., 1995; Williams, 1994; Braiman & Rothschild, 1988; Tamm & Talulian, 1993). Spectra of DAGK in oriented gel phase DPPC multilayers taken with parallel and orthogonally polarized incident light are shown in Figure 2C,D. The α-helical component of the Fourier self-deconvolution of the DAGK spectrum exhibits a high dichroic ratio of 3.3 ± 0.2. Similar results were obtained from DAGK in L_α-phase POPC, indicating little dependence of the structure of DAGK upon the phase of the host lipid matrix.

The dichroic ratio of 3.3 leads to calculation of helical order parameters of 0.37−0.67 if the range of transition moment orientations reported in the literature is used (see Materials and Methods). Figure 4 offers some insight into the structural usefulness of this data. This figure can be conservatively interpreted to make two important points. First, for multihelical proteins ATR-IR order parameters do not generally lead to a unique solution of helical orientations. Nevertheless, such data can be used to support or refute given models. In the case of DAGK, it is notable that the observed order parameters are consistent with a range of structures in which the three TM helices are well-aligned with the bilayer normal (0−10° tilt), while the two amphipathic helices are roughly aligned (0−40°) with the bilayer *plane*. This range of models is consistent with additional considerations. First, none of the three transmembrane helices have hydrophobic stretches which are longer than ca. 23 residues and thus should be just long enough to span the cytoplasmic membrane in near-0° orientations. Secondly, assuming that the second amphipathic helix is initiated at serine 74 and runs for at least 16 residues, the small number of flanking residues linking it to TM segments 2 and 3 should constrain the helix

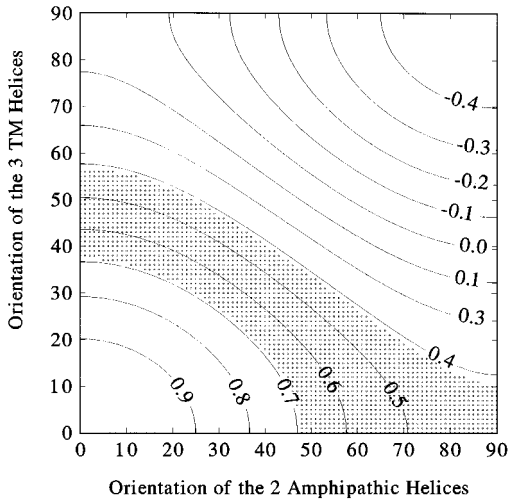

FIGURE 4: Calculated ATR-IR helical order parameters for a protein containing three transmembrane and two amphipathic helices (see eq 2). It has been assumed that all five helices have the same length, that the three TM helices share the same orientation, and that the amphipathic helices share another orientation. The angles for the helical axes are with respect to the bilayer *normal*. The gray area of the plot represents combinations of orientations which are consistent with the observed range of order parameters (0.37−0.67).

to the proximity of the bilayer surface. The helical orientations illustrated in Figure 3 reflect this model.

DAGK Can Spontaneously Insert into Preformed Unilamellar Vesicles from a Micellar Solution. It has previously been demonstrated that a number of membrane proteins will spontaneously insert into lipid vesicles from micellar solutions (Scotto & Gompper, 1990; Scotto & Zakim, 1988). The enzymic activity of DAGK provided us with a convenient means to monitor for *catalytically productive* insertion. Large (100 nm) unilamellar POPC vesicles which had been doped with a fluorescently tagged diacylglycerol (PBBG, see Materials and Methods) were used for the insertion studies. At 20 °C these vesicles are in the liquid crystalline phase.

Into the POPC-PBBG vesicular solutions small volumes of DAGK in 20 mM decyl maltoside (DM) were diluted by a factor of 200−250 such that the final detergent/POPC ratio was ≤1:250. Since the critical micelle concentration of DM is about 2 mM, the DM concentrations in the final reaction mixtures were about 20 times below CMC. At such low levels DM would not be expected to disrupt bilayers. This point and the improbability that micellar DM would disrupt the bilayers during the short (<2 s) mixing time during which the micelles were dissolved in the vesicular solutions are supported by the fact that decyl maltoside is not a very effective solubilizing agent for POPC bilayers. We observed that addition of 3 volumes of 20 mM decyl maltoside solution to 1 volume of POPC (25 mM) vesicles failed to produce detectable clarification of the opalescent POPC solution. Lack of disruption of the vesicles is also supported by the fact that DAGK was unable to phosphorylate PBBG located in the inner lipid leaflet of the vesicles (see below).

Figure 5A provides an example of a TLC assay for a standard mixed *micellar* reaction in which micellar DAGK was added to PBBG-containing mixed micelles. Such data were used to measure the initial rates of the DAGK reaction in both micelles and in vesicles (see Materials and Methods). As can be observed in Figure 5A, when the *micellar* reaction reaches equilibrium, the concentration of PBBG is so low as to be undetectable. Analogous assays were carried out in which micellar DAGK was added to POPC vesicles.

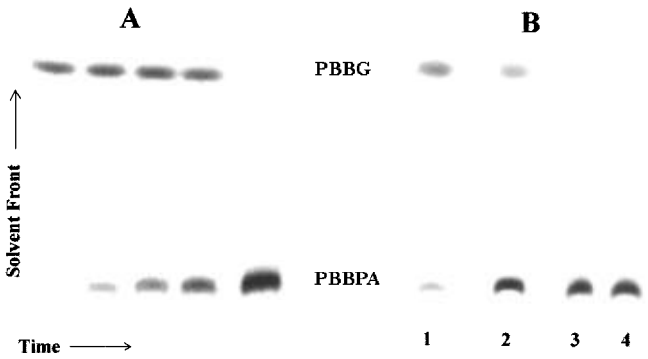

FIGURE 5: Examples of thin layer chromatograms used to assay DAGK's phosphorylation of pyrene-tagged DAG in mixed micelles and in vesicles (gray-scale photographic negatives of images which were originally light blue spots on a black background under near-UV light). (A) Progress of a mixed micellar DAGK reaction run to completion. (B) DAGK reaction in which 10 μL of 43 units/mL DAGK in 21 mM DM was added to 0.2 mL of POPC vesicles (25 mM POPC) containing 5 mol % PBBG. The first lane represents a time point during the reaction just after the addition of DAGK (well before equilibrium). Lane 2 represents reaction once it has reached an apparent equilibrium under conditions in which the vesicles are still intact. The third and fourth lanes represent the final equilibrium mixture *after dissolving the vesicles* by adding 75 μL of 0.34 M octyl glucoside.

Unlike the micellar reactions, we observed that substantial PBBG inevitably remained when the vesicular reactions were brought to apparent equilibrium by addition of a small aliquot of concentrated DAGK (1−2 μL of 150 units/mL). The most likely explanation for why some PBBG remained unreacted in unilamellar vesicles is that it was located on the inner leaflets where it could not be phosphorylated by DAGK. To test this interpretation, we allowed a vesicular reaction to reach apparent equilibrium, quantitated the amounts of PBBG and PBBPA present, and then dissolved the vesicles using octyl glucoside and checked to see whether the PBBG from the micellized vesicles was now susceptible to DAGK phosphorylation. This was observed to be the case (Figure 5B). This result strongly supports the assertion that detergent from the DAGK stock solution was not disrupting the lipid vesicles, which would have permitted all of the inner leaflet PBBG to be phosphorylated by DAGK.[1]

The specific activity of DAGK inserted into POPC or POPC-cardiolipin bilayers from micellar stock solution as reported in Table 1 was ca. 30% that observed in mixed micelles.[2] This indicates a high efficiency of productive insertion of DAGK from a diluted micellar solution into vesicles.

The results of this section cannot completely rule out the possibility that detergent may be involved in the insertion

[1] At first glance this might also appear to indicate that DAGK insertion is vectorial such that it does not functionally orient in both directions (placing functioning active sites at both inner and outer lipid−water interfaces). However, such an interpretation cannot be made because the amount of ATP trapped within the vesicles can be calculated to be insufficient to permit stoichiometric conversion of inner leaflet PBBG to PBBPA even if DAGK's active site reached that leaflet.

[2] This assumes that V_{max} for DAGK in lipid vesicles is the same as V_{max} in mixed micelles. This is reasonable based on two pieces of evidence: (i) DAGK's V_{max} is known to be rather insensitive to the specific types of lipids and detergents used in mixed micellar assays (Walsh and Bell, 1986a,b; Sanders et al., unpublished), and (ii) assays have been carried out using micelle-like bilayered fragments "bicelles", see Sanders and Landis (1995)] in which the rate has observed to be the same as in conventional mixed micelles at the similar substrate concentrations (unpublished).

Table 1: DAGK Activity under Various Assay Conditions

DAGK stock solution	reaction medium[a]	DAGK activity[b] (units/mg)
DM micelles	DM-DMPC mixed micelles coupled assay, 30 °C	15 ± 2 (many)
DM micelles	DM-DMPC mixed micelles	16 ± 5 (6)
DM micelles	POPC unilamellar vesicles	4.3 ± 2.8 (3)
DM micelles	POPC ULV containing 5 mol % cardiolipin	5.2 ± 2.1
8 M urea + sub-CMC DM	DM-DMPC mixed micelles coupled assay, 30 °C	8 ± 3
8 M urea + sub-CMC DM	POPC unilamellar vesicles (L_α)	1.4 ± 0.9[c] (2)
8 M urea + sub-CMC DM	DPPC unilamellar vesicles, 20 °C (gel)	0.015 ± 0.01[d]
8 M urea + sub-CMC DM	DPPC unilamellar vesicles, 50 °C (L_α)	0.7 ± 0.5
6.5 M urea, no detergent	DM-DMPC mixed micelles coupled assay, 30 °C	7.2 ± 3.4 (5)
6.5 M urea, no detergent	DM-DMPC mixed micelles	3.4 ± 1.4
6.5 M urea, no detergent	POPC unilamellar vesicles (L_α)	0.61 ± 0.33 (7)

[a] Containing 5 mol % PBBG, buffered as described in Materials and Methods at pH 6.7 and 22 ± 2° C unless otherwise noted. [b] DAGK was quantitated based on absorbance at 280 nm. The number in parentheses is the number of times the rate was actually measured (if no parentheses, 1 trial). One Unit of DAGK activity = 1 μmol of DAG phosphorylated per min. In cases where only a single measurement was made, the standard deviations are conservatively assumed to be rather large: ±40% for the TLC/fluorescent assay and ±14% for the coupled assay. [c] The DAGK/urea stock solution contained 0.3 mM DM such that the detergent concentrations in the final reaction mixtures represented by these rates were ≤0.02 mM (100× below CMC and 1:1000 DM/lipid). [d] The assay method used does not permit us to distinguish whether this very low activity in the gel phase vesicles reflects a reduction in the degree of insertion and/or whether it reflects a lower V_{max} for correctly inserted enzyme.

process either during the mixing time prior to protein−detergent micelle dissolution or after mixing (perhaps via tightly DAGK-associated detergent). This consideration led to the studies of next sections.

DAGK Can Be Solubilized and Refolded in Mixed Micelles from Urea Solutions. Two different methods were used to solubilize DAGK in concentrated urea solutions. First, lyophilized DAGK-DM powder was dissolved by a amphiphile-free 8 M urea solution such that the DM concentration was 7× below its CMC. Under these conditions the enzyme was fully soluble. That solubility was maintained by urea and not by the residual DM was verified by the observation that DAGK precipitates from DM solutions when diluted into urea-free buffer such that the DM concentration is 7× below CMC. Other urea/DAGK stock solutions were prepared by complete delipidation. A 1 mL Ni^{2+}-agarose column onto which pure DAGK was bound through its polyHis tag was washed successively with 12 × 1 column volumes of 6.5 M urea in neutral buffer and in the absence of detergent to completely strip the enzyme of associated detergent and lipid. DAGK was then eluted from the column with 6.5 M urea plus 2% formic acid to yield fully soluble DAGK.

The DAGK in these stock solutions is effectively inactive but does maintain some α-helical secondary structure. We ran a fluorescent-TLC assay in 4.4 M urea and found that even in the presence of mixed micelles, DAGK's specific activity was observed to be only 0.06 unit/mg: a 250-fold loss of activity. At higher urea concentrations and in the absence of significant concentrations of detergent and/or lipid, it is reasonable to assume that the activity would be effectively 0. Nevertheless, CD studies carried out in the Bowie lab (unpublished) indicate a largely helical secondary structure for DAGK in 8 M urea, indicating that while tertiary structure is almost certainly gone, DAGK persists in maintaining considerable secondary structure.

The urea solutions containing DAGK were assayed by diluting small aliquots (usually 10 μL) into the standard 1 mL coupled-UV assay (see Materials and Methods) involving mixed micelles of octyl glucoside and dimyristoyl-PC. As summarized in Table 1, the specific activities from the DAGK/urea stock solutions were roughly 50% of the rate observed using micellar stock DAGK solutions. This recovered activity indicates that DAGK *refolding* from urea solutions is relatively efficient in the presence of mixed micelles.

Insertion of Urea-Solubilized DAGK into Lipid Vesicles. One to ten microliter aliquots of the urea-solubilized DAGK solutions described above were added to 0.15−0.25 mL solutions containing POPC vesicles with PBBG, and the reaction rates were measured. It is known that even high concentrations of urea do not disrupt lipid vesicles (Oku & MacDonald, 1983a,b), and so the presence of up to 0.5 M urea should not provide an undesired pathway for DAGK insertion. As noted above, DAGK/urea stock solutions were prepared by two different methods, one in which a small quantity of residual detergent was present and one which removes all detergent and lipid. The measured rates are given in Table 1 and are in the range of 1.5−10% relative to the rates observed for mixed micellar assays of DAGK from *micellar* stock solutions.

We considered the possibility that spontaneous DAGK insertion might be enhanced by factors specifically related to the use of 100 nm vesicles which have a somewhat smaller radius of curvature than the cytoplasmic membrane of *E. coli*. To test this possibility, we compared the degree of incorporation of DAGK into 50 nm vesicles relative to 100 nm vesicles. Reactions were run with using a single lipid/detergent-free DAGK/urea stock solution and using vesicles prepared from the same batch of POPC/PBBG powder. Two reactions were run for each vesicle size. The average specific activity measured for the smaller vesicles (0.51 ± 0.15 unit/mg) was actually lower than for the larger vesicles (1.1 ± 0.4 unit/mg). The fact that DAGK insertion into the larger of the vesicles indicates that DAGK insertion is not promoted by bilayer defects related to surface curvature.

Finally, we considered whether the observed efficiency of productive insertion reflects a *thermodynamic* equilibrium between productive and nonproductive states or whether it represents partitioning of the enzyme between competing *kinetic* pathways to effectively irreversible states. Table 1 demonstrates that the observed efficiency was higher by a factor of 5−10 when DAGK was diluted into vesicles from detergent solution relative to dilution from urea solutions, despite the fact that the final reaction conditions are effectively identical. This observation appears to rule out the thermodynamic interpretation. The "“nonproductive” kinetic pathway for DAGK is probably irreversible aggrega-

Table 2: Properties of Purified DAGK Mutants[a]

mutant DAGK	precipitate forms?[b]	DAGK conc. (mg/mL)[d]	DAGK activity (units/mg)[d]
A1D,N3F,T4I,T5S,G6C,F7L	no	9.8	0.5
A1D,T4Y,F7C,T8A,K12R	no	9.4	7.3
W18C,R22H,A23T	no	8.1	2.9
R22C,I26N	no	16	16
S17C,W18L,G20V,A23S	no	5.4	0
Q33T, L40M,I44C	yes	7.9	0.7
G35F,A37C,V43G,A45V	yes	6.8	0
A30P,F31C,V38F,L40V,V42L, V43L,A45S	yes	6.2	0
R32G,Q33L,G35C,V36A,V42F	yes	10	0.03
A37G,L40M,I44C	yes	7.0	0.59
C46I,W47S,V50A,R55C	yes	4.4	0
V62L,V68F,A74C	yes	8.3	0
S84C	no	16	3.3
Y86S,H87L,L89M,S90C	no	10	0.08
E88A,S90C	yes	9.7	0

[a] All of the mutants yielded 50−100% of the activity of wild-type DAGK in a phenotypical assay (Wen et al., 1996). [b] Within 2 h after purification at 4° C. [c] In cases where a precipitate formed, DAGK absorbance was measured after the precipitate was removed by centrifugation. [d] The limit of detectability for the assay used (coupled spectrophotometric) is 0.015 U/ml (1000-fold dynamic range).

tion. It was observed that when urea-solubilized DAGK was diluted into vesicle-free buffer, it formed a visible aggregate which was not redissolved upon addition of detergent. Aggregation also explains the ca. 50% loss of activity when urea-solubilized DAGK is diluted into mixed micelles where there is no barrier to "insertion".

Use of Mutants to Probe the Mechanism of DAGK Insertion in Vivo. The pathway by which DAGK is properly inserted and refolded into the cytoplasmic membrane *in vivo* is not known. DAGK has no cleavable signal sequence and would not appear to require the *Sec* pathway because of its lack of a substantial periplasmic domain (Von Heijne, 1994; Wickner et al., 1991). The observation made in the above section that DAGK can spontaneously insert into model vesicles leads to the question of whether an analogous mechanism might be operative *in vivo*. The availability of mutant forms of DAGK offers a test of this possibility. If DAGK mutants could be identified which insert efficiently *in vivo* which do not insert with even modest efficiency in model systems then the pathways available for *in vivo* insertion must be more complicated than implied by the model studies.

Wen et al. (1996) have described work in which a large library of mutant DAGKs were cloned into an *E. coli* mutant (RZ6; Raetz & Newman, 1976) in which the wild-type DAGK was knocked out. In the absence of a functioning DAGK this phenotype will not grow under conditions of low osmolarity. Thus, when a mutant DAGK is expressed its folding, insertion, and catalytic viability can be readily assessed. A substantial percentage of the roughly 250 mutants supported RZ6 culture growth in low osmolarity medium which was at least 50% as efficient as growth in the presence of expressed wild-type DAGK (Wen et al., 1996). We obtained a number of the mutant-harboring strains and purified the DAGKs using the standard polyHis tag-based method, yielding DM micellar solutions of the mutants.

Wild-type DAGK remains fully active (15 unit/mg) in decyl maltoside solutions for many hours at room temperature, and 15 mg/mL solutions exhibit little visible aggregate formation with time. While all of the mutants examined were able to support RZ6 cell growth in low osmolarity media (Wen et al., 1996) and while all eluted as initially clear solutions from the Ni-agarose columns, a number of the mutants formed visible aggregates in decyl maltoside solutions after sitting for a few minutes at room temperature. Some mutants also failed to exhibit detectable DAGK activity. In general, propensity to visibly aggregate was correlated with a lack of activity. In cases where aggregation was observed, the precipitate was removed by centrifugation, and the supernatant was assayed for DAGK content by absorbance at 280 nm and DAGK activity. In such cases we generally observed that while substantial DAGK remained in solution, it was not active. Data for a number of these mutants are summarized in Table 2. These results suggest that while all of the mutants examined can apparently fold and correctly insert *in vivo* to produce catalytically viable DAGK, extraction of some mutants into a micellar solution results in irreversible aggregation and/or misfolding.

These results demonstrate that mutations in the sequence of DAGK can dramatically attenuate the differences between the refolding/insertion efficiency *in vivo* versus *in vitro*. This observation appears to highlight mechanisms available in *E. coli* to facilitate proper DAGK folding and insertion which are not present in simple micellar and vesicular solutions.

DISCUSSION

The FT-IR spectroscopic measurements made in this paper extend our knowledge of DAGK's bilayer-associated structure beyond its simple topological map by demonstrating that it is a largely α-helical protein. The next logical steps are to establish its functional oligomeric state and how its helices pack together in bilayers.

The bilayer insertion studies of this paper demonstrated that DAGK can spontaneously insert into lipid vesicles and adopt its functional structural state fairly efficiently, even from lipid/detergent-free solutions. However, the experiments with DAGK mutants indicated that the mechanism for insertion into the cytoplasmic membrane of *E. coli* under biosynthetic conditions is probably more complicated than implied by the model bilayer experiments. This observation is not surprising given the plethora of phenomena related to protein folding, membrane insertion, and membrane translocation in *E. coli* (Gennis, 1989; Wickner et al., 1991; von Heijne, 1994; Cao et al., 1994; Popot et al., 1994; Saier, 1994; Zen et al., 1995; Schatz & Dobberstein, 1996).

Regardless of the *in vivo* route by which DAGK enters its native membrane, the model bilayer insertion results are of significance because they provide a rough experimental measurement of the energy barrier to DAGK refolding and insertion. A conservative estimate of the minimum observed efficiency of DAGK insertion into lipid vesicles is represented by the average insertion efficiency observed for DAGK from lipid/detergent free urea solutions minus the standard deviation of the measurements (Table 1): 3.8% − 2.1% = 1.7%. As explained in the Results, this efficiency appears to reflect patitioning of DAGK between competing kinetic pathways leading to effectively irreversible final states. Accordingly, an efficiency of ≥1.7% corresponds to a maximum difference in the standard free energies of activation ($\Delta\Delta G^{\ddagger}$) between the productive and nonproductive pathways of <4 kcal/mol. Since the rate barrier for the nonproductive process (most likely aggregation) is probably

very low, this result indicates that the energy barrier to productive insertion of DAGK in bilayers is quite modest. This result is of relevance to an on-going discussion on the energetics of membrane protein folding and insertion (cf. Engelman & Steitz, 1981; Jahnig, 1983; Jacobs & White, 1989; Moll & Thompson, 1994; Ben-Tal et al., 1996).

Our conclusion that the energy barrier for DAGK insertion into bilayers is rather small is similar to conclusions which can be drawn for at least two other polytopic membrane proteins. Surrey and Jahnig (1992) reported spontaneous insertion of the OmpA porin from urea solutions into preformed lipid vesicles with an efficiency of 40−50%. More recently, Soekarjo et al. (1996) demonstrated that the M13 precoat protein can spontaneously insert into preformed vesicles from diluted organic solvent mixtures such that about 20% of the protein transverses the membrane. Like DAGK, the M13 precoat and the OmpA porin contain polar residues which are translocated across the membrane in the process of folding and insertion. However, the largely β-sheet OmpA differs from the α-helical DAGK and M13 precoat in that it inserts only into *small* unilamellar vesicles.

The results of this work do not allow us to assess the molecular details of the spontaneous bilayer insertion for DAGK. However, the prospects for elucidating this process are promising based on the methods described in this paper and the availability of a substantial library of DAGK mutants (Wen et al., 1996), particularly if the structural progress described in this paper can be extended to tertiary and quaternary levels.

ACKNOWLEDGMENT

We are grateful to Jim Bowie and to his lab for providing us with wild-type and mutant DAGK-overexpressing strains of *E. coli*, for a lively dialogue regarding the practical aspects of working with DAGK, and for a providing us with a preprint of Wen et al. (1996). We also thank Tom Woolf (Johns Hopkins University) for helpful discussion and Lily Fisher (Yale University) for assistance with a number of the IR experiments.

REFERENCES

Adams, G. A., & Rose, J. K. (1985) *Cell 41*, 1007−1015.
Arkin, I. T., Rothman, M., Ludlam, C. F. C., Aimoto, S., Engelman, D. M., Rothschild, K. J., & Smith, S. O. (1995) *J. Mol. Biol. 248*, 824−834.
Axelsen, P. H., Kaufman, B. K., McElhaney, R. N., & Lewis, R. N. A. H. (1995) *Biophys. J. 69*, 2770−2781.
Bell, R. M., & Hjelmstad, R. H. (1991) *Biochemistry 30*, 1731−1740.
Ben-Tal, N., Ben-Shaul, A., Nicholls, A., & Honig, B. (1996) *Biophys. J. 70*, 1803−1812.
Bradbury, E. M., Brown, L., Downie, A. R., Elliot, A., Fraser, R. D. B., & Hanby, W. E. (1962) *J. Mol. Biol. 5*, 230−247.
Braiman, M. S., & Rothschild, K. J. (1988) *Annu. Rev. Biophys. 17*, 541−570.
Cao, G., Cheng, S., Whitley, P., von Heijne, G., Kuhn, A., & Dalbey, R. E. (1994) *J. Biol. Chem. 269*, 26898−26903.
Engelman, D. M., & Steitz, T. A. (1981) *Cell 23*, 411−422.
Fasman, G. D. (1995) *Biopolymers 37*, 339−362.
Frey, S., & Tamm, L. K. (1991) *Biophys. J. 60*, 922−930.
Geller, B. L., & Wickner, W. (1985) *J. Biol. Chem. 260*, 12381−13285.
Gennis, R. B. (1989) *Biomembranes: Molecular Structure and Function*, Springer-Verlag, New York.
Harper E. T., & Rose, G. D. (1993) *Biochemistry 32*, 7605−7609.
Harrick, N. J. (1967) *Internal Reflection Spectroscopy*, Interscience Publishers, New York.
Jacobs, R. E., & White, S. H. (1989) *Biochemistry 28*, 3421−3437.
Jahnig, F. (1983) *Proc. Natl. Acad. Sci. U.S.A. 80*, 3691−3695.
Kauppinen, J. K., Moffatt, D. J., Mantsch, H. H., & Cameron, D. G. (1981) *J. Appl. Spectrosc. 35*, 271−276.
Kodali, D. R., & Duclose, R. I. (1992) *Chem. Phys. Lipids 61*, 169−173.
Lewis, B. A., & Engelman, D. M. (1983) *J. Mol. Biol. 166*, 211−217.
Moll, T. S., & Thompson, T. E. (1994) *Biochemistry 33*, 15469−15482.
Oku, N., & MacDonald, R. C. (1983a) *J. Biol. Chem. 258*, 8733−8738.
Oku, N., & MacDonald, R. C. (1983b) *Biochim. Biophys. Acta 734*, 54−61.
Popot, J.-L., De Vitry, C., & Atteia, A. (1994) in *Membrane Protein Structure* (White, S. H., Ed.) pp 41−96, Oxford, New York.
Raetz, C., & Newman, K. (1978) *J. Biol. Chem. 253*, 3882−3887.
Rand, R. P., & Parsegia, V. A. (1989) *Biochim. Biophys. Acta 988*, 351−376.
Reithmeier, R. A. F. (1995) *Curr. Opin. Struct. Biol. 5*, 491−500.
Russ, E., Kaiser, U., & Sandermann. (1988) *Eur. J. Biochem. 171*, 335−342.
Saier, M. H. (1994) *Microbiol. Rev. 58*, 71−93.
Sanders, C. R., & Schwonek, J. P. (1993) *Biophys. J. 65*, 1207−1218.
Sanders, C. R., & Landis, G. C. (1995) *Biochemistry 34*, 4030−4040.
Schatz, G., & Dobberstein, B. (1996) *Science 271*, 1519−1526.
Scotto, A. W., & Zakim, D. (1988) *J. Biol. Chem. 263*, 18500−18506.
Scotto, A. W., & Gompper, M. E. (1990) *Biochemistry 29*, 7244−7251.
Smith, R. L., O'Toole, J. F., Maguire, M. E., & Sanders, C. R. (1994) *J. Bacteriol. 176*, 5459−5465.
Soekarjo, M., Eisenhower, M., Kuhn, A., & Vogel, H. (1996) *Biochemistry 35*, 1232−1241.
Surewicz, W., Mantsch, H. M., & Chapman, D. (1993) *Biochemistry 32*, 389−394.
Surrey, T., & Jahnig, F. (1992) *Proc. Natl. Acad. Sci. U.S.A. 89*, 7457−7461.
Tamm, L. K., & Talulian, S. A. (1993) *Biochemistry 32*, 7720−7726.
Tsuboi M. (1962) *J. Polym. Sci. 59*, 139−153.
Venyaminov, S. U., & Kalnin, N. N. (1990a) *Biopolymers 30*, 1243−1257.
Venyaminov, S. U., & Kalnin, N. N. (1990b) *Biopolymers 30*, 1259−1271.
von Heijne, G. (1994) in *Membrane Protein Structure* (White, S. H., Ed.) pp 27−40, Oxford, New York.
Walsh, J. P., & Bell, R. M. (1986a) *J. Biol. Chem. 261*, 15062−15069.
Walsh, J. P., & Bell, R. M. (1986b) *J. Biol. Chem 261*, 6239−6247.
Walsh, J. P., & Bell, R. M. (1992) *Methods Enzymol. 209*, 153−162.
Walsh, J. P., Fahrner, L., & Bell, R. M. (1990) *J. Biol. Chem. 265*, 4374−4381.
Wen, J., Chen, X., & Bowie, J. (1996) *Nature, Struct. Biol. 3*, 141−147.
Wickner, W., Driessen, A. J. M., & Hartl, F.-U. (1991) *Annu. Rev. Biochem. 60*, 101−124.
Williams, R. W. (1994) in *Membrane Protein Structure* (White, S. H., Ed.) pp 181−205, Oxford, New York.
Yamashita, Y., Takehara, T., & Kuramitsu, H. K. (1993) *J. Bacteriol. 175*, 6220−6228.
Zen, K. H., Consler, T. G., & Kaback, H. R. (1995) *Biochemistry 34*, 3430−3437.

BI9604892